Passive PT-Symmetric Metasurfaces With Directional Field Scattering Characteristics

Nicholas S. Nye, Ahmed El Halawany, Ahmed Bakry, M. A. N. Razvi, Ahmed Alshahrie, Mercedeh Khajavikhan, and Demetrios N. Christodoulides

***Abstract*—We show that passive parity-time (PT) symmetric metasurfaces can be utilized to appropriately engineer the resulting far-field characteristics. Such PT-symmetric structures are capable of eliminating diffraction orders in specific directions, while maintaining or even enhancing the remaining orders. A systematic methodology is developed to implement this class of metasurfaces in both one-dimensional and two-dimensional geometries. In two-dimensional systems, PT symmetry can be established by employing either H-like diffractive elements or diatomic oblique Bravais lattices.**

***Index Terms*—Directional scattering, metasurfaces, PT-symmetry.**

I. Introduction

RECENTLY, there has been considerable interest in synthesizing optical structures and devices that simultaneously exploit the presence of gain and loss domains, while maintaining parity time (PT) symmetry [1]–[14]. PT symmetry first emerged within the context of quantum field theories after recognizing that a special class of non-Hermitian Hamiltonians can exhibit entirely real eigenvalue spectra, as long as they commute with the antilinear PT operator. In general, a necessary (but not sufficient) condition for PT-symmetry to hold is that the complex potential involved in such Hamiltonians should obey $V(\boldsymbol{r}) = V^*(-\boldsymbol{r})$, which directly implies that the real part of the potential must be an even function of position, while the imaginary should be antisymmetric. Lately, such PT prospects have been proposed in the field of optics by recognizing that the complex refractive index distribution plays the role of an optical potential. In this case, PT-symmetry demands that $n(\boldsymbol{r}) = n^*(-\boldsymbol{r})$. This latter condition clearly indicates that the refractive index profile must be symmetric, whereas the imaginary component (signifying gain or loss) must be an odd function in coordinate space. In more general settings, where the problem must be treated electrodynamically, this same symmetry can be introduced provided that the complex permittivity now satisfies $\varepsilon(\boldsymbol{r}) = \varepsilon^*(-\boldsymbol{r})$ [14]. PT-symmetric optical arrangements can exhibit a number of exciting properties. These include for example power oscillations, non-reciprocal light propagation and Bloch oscillations [2]–[5], and unidirectional invisibility [12], [13] to mention a few.

In recent years, optical metasurfaces, a special class of metamaterials with reduced dimensionality, have also received considerable attention. Such artificial surfaces can effectively control the flow of light through appropriately engineered subwavelength, surface-confined features that can introduce abrupt phase discontinuities after light encounters the interface [15]–[18]. So far, several studies have successfully demonstrated the use of optical metasurfaces in manipulating and controlling the phase, polarization and angular momentum of the incident light [19]–[24].

In this paper we show that one-dimensional (1-D) and two-dimensional (2-D) optical metasurfaces endowed with PT-symmetry can display several intriguing characteristics. As we will see, PT-symmetry can be readily introduced in these systems through an appropriate amplitude and phase modulation when imposed on the surface. Even though bulk non-Hermitian gratings have been considered before in 1-D configurations [25]–[35], here we extend these concepts in more complex settings with particular emphasis on optical PT-symmetric metasurfaces. Such PT-symmetric structures are capable of eliminating diffraction orders in specific directions, while maintaining or even enhancing the remaining orders. In our study we provide all-passive 1-D and 2-D metasurface designs suitable for both the visible (532 nm) and NIR (1550 nm) bands. Such PT-symmetric metasurfaces can provide an alternative avenue to existing techniques [36]–[38] for effectively controlling a number of diffraction orders through surface-confined passive nano-features.

II. 1D Passive Pt-Symmetric Metasurfaces

A. Design Approach

To analyze the optical properties of a PT-symmetric metasurface, we assume that the complex refractive index $n(x) = f(x) + ig(x)$ is periodically modulated on the surface. Here $f(x)$ and $g(x)$ are periodic real functions having a spatial period L, representing the length of each unit cell on this metasurface. In this regard, $n(x)$ can be expressed through a Fourier series

Manuscript received December 21, 2015; revised February 10, 2016; accepted February 10, 2016. This work was supported by NSF CAREER Award No. ECCS-1454531, NSF under Grant ECCS-1128520, NSF under Grant DMR-1420620, AFOSR under Grant FA9550-14-1-0037, and also by the Deanship of Scientific Research, King Abdulaziz University under Grant 66-130-35-HiCi. The authors, therefore, acknowledge technical and financial support of KAU. The work of N. S. Nye was supported by the A. S. Onassis Public Benefit Foundation and the Foundation for Education and European Culture.

N. S Nye, M. Khajavikhan, and D. N. Christodoulides are with the College of Optics and Photonics, University of Central Florida, Orlando, FL 32816-2700, USA (e-mail: nnye@knights.ucf.edu; mercedeh@creol.ucf.edu; demetri@creol.ucf.edu).

A. El Halawany is with the Department of Physics and the College of Optics and Photonics, University of Central Florida, Orlando, FL 32816-2700, USA (e-mail: ahmedhalawany@knights.ucf.edu).

A. Bakry, M. A. N. Razvi, and A. Alshahrie are with the Physics Department, King Abdulaziz University, Jeddah 21589, Saudi Arabia (e-mail: abakry@kau.edu.sa; mrazvi@kau.edu.sa; aalshahri@kau.edu.sa).

Color versions of one or more of the figures in this paper are available online at http://ieeexplore.ieee.org.

Digital Object Identifier 10.1109/JSTQE.2016.2537798

as follows

$$n(x) = (a_0 + ia_0') + \frac{1}{2}\sum_{m=1}^{\infty}\left[(a_m + b_m') + i(a_m' - b_m)\right]e^{im\theta} + \frac{1}{2}\sum_{m=1}^{\infty}\left[(a_m - b_m') + i(a_m' + b_m)\right]e^{-im\theta} \quad (1)$$

where $\theta = 2\pi x/L$. In Eq. (1), $\{a_m, b_m\}$ and $\{a_m', b_m'\}$ represent the Fourier coefficients associated with the real $f(x)$ and imaginary $g(x)$ components of the complex refractive index distribution, respectively. The envisioned PT-symmetric metasurface is expected to be implemented solely using passive components, i.e., the imaginary component $g(x)$ will introduce only loss.

Of interest would be to identify methods through which the negative (or positive) diffraction orders emanating from this PT-symmetric metasurface can be entirely suppressed while the remaining orders (positive or negative) can be enhanced. For this to occur one has to eliminate, for example, the negative orders $\exp(-im\theta)$ appearing in the Fourier series of Eq. (1). This directly implies that $b_m' = a_m$ and $a_m' = -b_m$. From here, one obtains the following representations for $f(x), g(x)$ that are necessary to suppress the negative orders

$$f(x) = a_0 + \sum_{m=1}^{\infty}\left\{a_m\cos\left(m\frac{2\pi x}{L}\right) + b_m\sin\left(m\frac{2\pi x}{L}\right)\right\}$$
$$g(x) = a_0' + \sum_{m=1}^{\infty}\left\{a_m\sin\left(m\frac{2\pi x}{L}\right) - b_m\cos\left(m\frac{2\pi x}{L}\right)\right\}. \quad (2)$$

Equations (2) show that this is only possible as long as the real and imaginary parts of the refractive index are intertwined through common coefficients a_m, b_m. This index distribution is PT-symmetric, when the terms in Eq. (2) associated with the a_m, b_m coefficients are considered separately. Similarly, one can eliminate the positive orders $e^{im\theta}$ provided that $b_m' = -a_m$ and $a_m' = b_m$, in which case the following relations hold true

$$f(x) = a_0 + \sum_{m=1}^{\infty}\left\{a_m\cos\left(m\frac{2\pi x}{L}\right) + b_m\sin\left(m\frac{2\pi x}{L}\right)\right\}$$
$$g(x) = a_0' + \sum_{m=1}^{\infty}\left\{-a_m\sin\left(m\frac{2\pi x}{L}\right) + b_m\cos\left(m\frac{2\pi x}{L}\right)\right\}. \quad (3)$$

Equations (2), (3) indicate that, in order to eliminate either the negative or the positive orders, $f(x)$ and $g(x)$ must be PT-symmetric partners. The diffractive configuration considered here, essentially acts like a phase screen with a phase transmission function of the form $\exp(ik_0 n(x)d)$, where d represents an effective depth. Equations (1)–(3) provide a methodology for designing such unidirectional metasurfaces. Once the subwavelength surface elements are positioned on the surface in a PT-symmetric fashion, finite element simulations (FEM) are then used to further optimize the performance of this arrangement.

In general the allowed diffraction orders associated with this metasurface system can be determined from $\vec{k}_{diff,tan} = \vec{k}_{inc,tan} + m\vec{G}_{lat}$, where $\vec{G}_{lat}$ is the reciprocal lattice vector of this 1-D lattice, and $\vec{k}_{inc,tan}$ and $\vec{k}_{diff,tan}$ are the tangential components of the incident and diffracted wave vectors, and m is the diffraction order. Since we are investigating this system in transmission mode, the previous relation implies that $n_2\sin\beta_m = n_1\sin\alpha + m(\lambda_0/L)$, where n_1, n_2 are the refractive indices of the incident and transmitted media, α is the angle of incidence, β_m is the diffraction angle and λ_0 is the free space wavelength.

B. PT-Symmetric Designs

Based on the aforementioned analysis we investigate the optical properties of the structures shown in Figs. 1, 2 for the wavelengths of 1550 and 532 nm, respectively. These configurations were conceived by matching the Fourier coefficients in a discrete fashion. These systems were subsequently optimized using finite element methods. For the 1550 nm design (see Fig. 1) we employ silicon as the transparent material and nickel for loss. On the other hand, the 532 nm design (see Fig. 2) is based on sapphire (as the transparent medium) and again utilizes nickel for loss. In general, the real part of the refractive indices of the transparent and lossy materials are here approximately equal in order to satisfy the PT-symmetry condition. We would like to note that, while the imaginary component in our designs is not exactly antisymmetric, their response is still dictated to a great extent by PT symmetry. This is due to the fact, that PT symmetric related processes can be quite robust and hence can tolerate environments, where this symmetry is not exactly satisfied. For both wavelengths, we assume normal incidence and a TE-polarization, i.e., the electric field is parallel to the 1-D stripes of this metasurface. Under these conditions, the designs shown in Figs. 1 and 2 support up to six transmission orders.

In order to evaluate the performance of these configurations, we consider an extinction ratio, defined as the ratio between the diffraction efficiencies associated with the positive orders to that of the negative orders and vice versa. The FEM results corresponding to the aforementioned structures are shown in Figs. 1, 2. As expected, if no loss is incorporated in the system (Hermitian case), light propagates symmetrically after this metasurface, as shown in Figs. 1(c), 2(c). In this case the positive and negative orders are exactly the same. This scenario changes once loss from nickel is introduced. The resulting field distributions and Poynting vector plots are shown in Figs. 1(d), 2(d). Under these conditions, the light is skewed in one direction, towards the lossy side. The physical reason behind this symmetry-breaking behavior has to do with the redistribution of energy flow within the system. In other words, the Poynting vector now develops an additional transverse component that is needed to supply energy to the lossy domains. For the 1550 nm design, the FEM

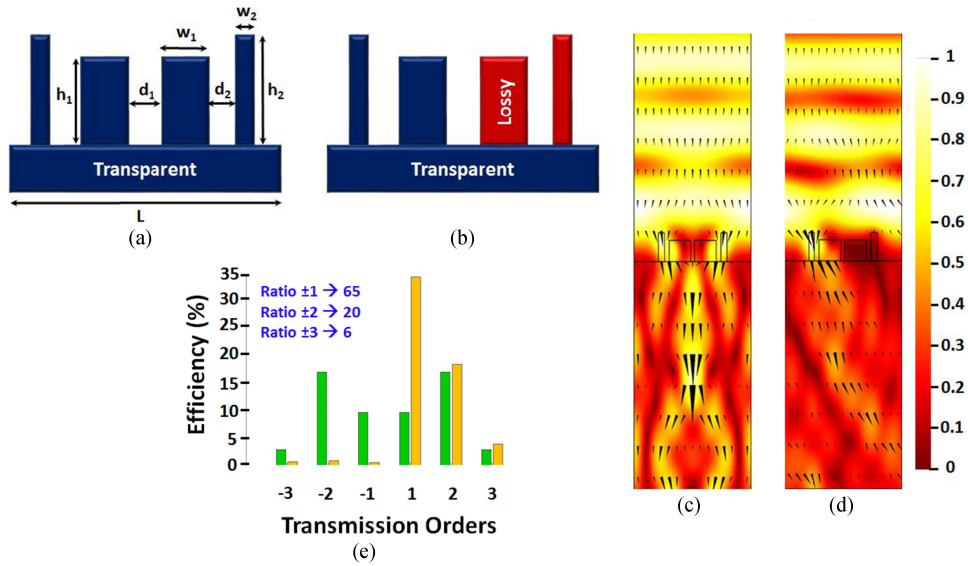

Fig. 1. 1-D metasurface design for 1550 nm with dimensions $L = 1520\,nm$, $h_1 = 230\,nm$, $h_2 = 310\,nm$, $w_1 = 280\,nm$, $w_2 = 80\,nm$, $d_1 = 50\,nm$, $d_2 = 60\,nm$. The transparent material is silicon with a refractive index $n_{Si} = 3.4757$ [38], while the lossy medium used is nickel with a refractive index $n_{Ni} = 3.4378 - 6.7359i$ [39]. (a), (c) Hermitian case (when no loss is incorporated) and corresponding near-field and Poynting vector (arrow plots), (b), (d) PT-symmetric case (when loss is introduced) and corresponding near-field and Poynting vector distributions, (e) transmission order efficiencies for the Hermitian case (green) and PT-symmetric case (yellow) and extinction ratios between the positive and corresponding negative orders (blue).

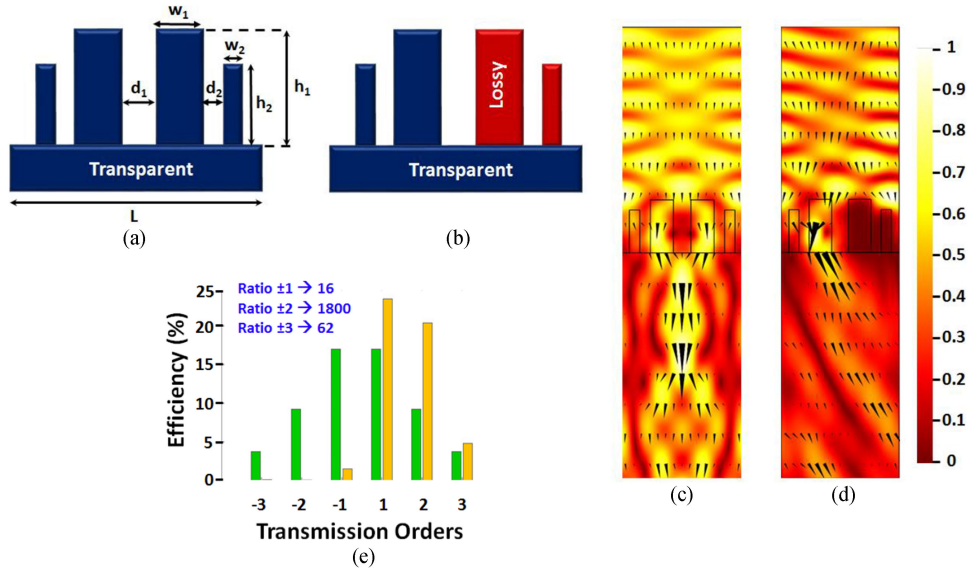

Fig. 2. 1-D metasurface design for 532 nm with dimensions $L = 1050\,nm$, $h_1 = 470\,nm$, $h_2 = 380\,nm$, $w_1 = 200\,nm$, $w_2 = 90\,nm$, $d_1 = 150\,nm$, $d_2 = 90\,nm$. The transparent material is sapphire with refractive index $n_{Al2O3} = 1.7718$ [40], while the lossy material is nickel with refractive index $n_{Ni} = 1.7764–3.776i$ [39]. (a), (c) Hermitian case (when no loss is incorporated) and corresponding near-field distribution and Poynting vector (arrow plots), (b), (d) PT-symmetric case (when loss is introduced) and corresponding near-field distribution and Poynting vector plot, (e) transmission order efficiencies for the Hermitian case (green) and PT-symmetric case (yellow) and extinction ratios between the positive and corresponding negative orders (blue).

simulations show that the extinction ratio between the ± 1 orders is approximately 65 (18 dB), for the ± 2 is 20 (13 dB) and for the ± 3 the extinction ratio is approximately 6 [see Fig. 1(e)]. On the other hand, the design intended for 532 nm exhibits optimum performance for the ± 2 orders where the extinction ratio is 1800 or 33 dB. Meanwhile for the remaining two orders it ranges between 62 to 16 [see Fig. 2(e)]. In essence, these metasurface designs can effectively suppress the positive (negative) orders by exploiting the symmetry-breaking induced by PT symmetry.

III. 2-D Passive PT-Symmetric Metasurfaces

A. Design Approach

Following a rationale similar to that used in the 1-D case, in order to identify designs capable of eliminating diffraction

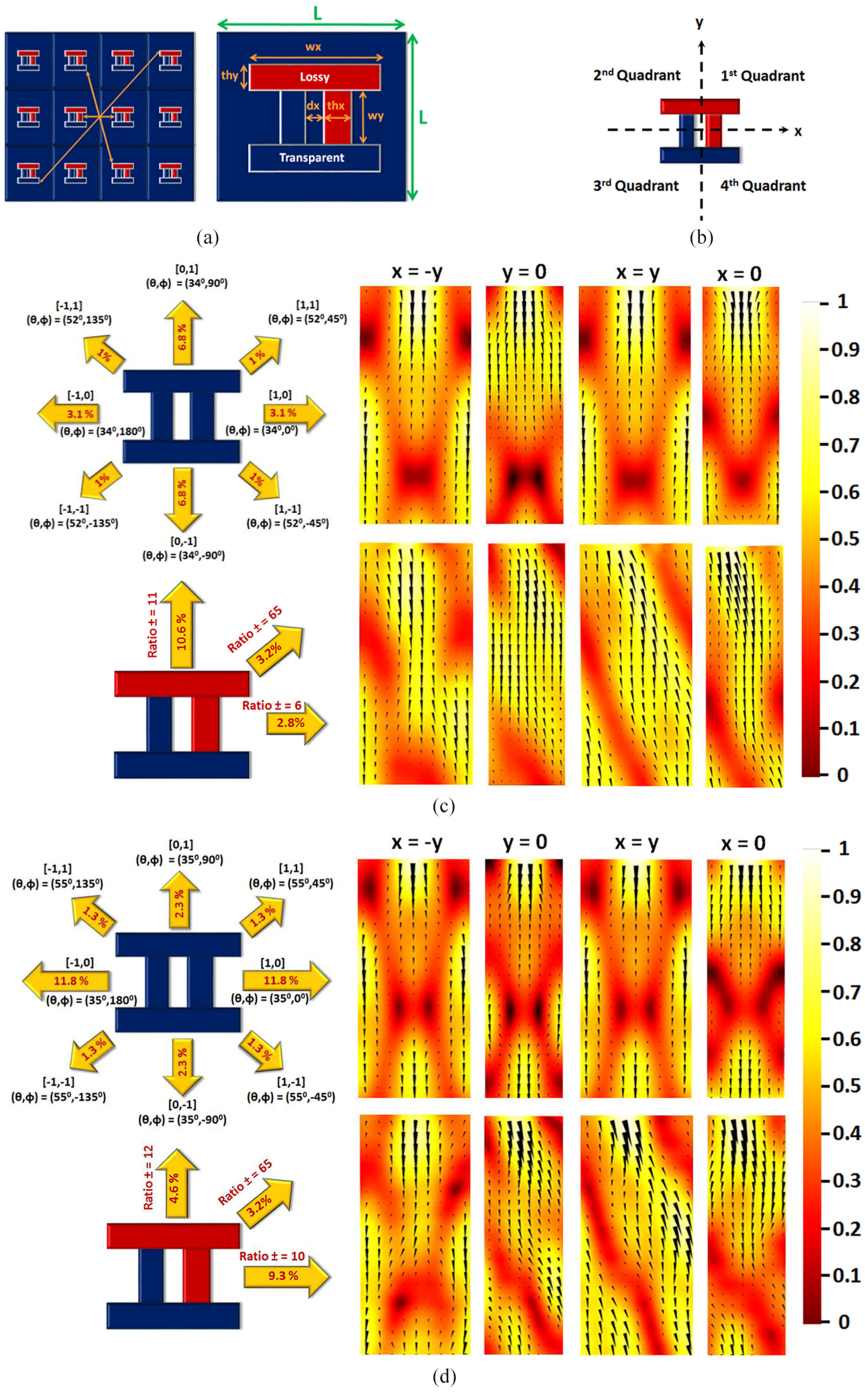

Fig. 3. H-like design: (a) H-element and corresponding lattice, (b) coordinate plane and quadrants, (c) FEM results of the transmission order efficiencies, normalized near-field distributions and Poynting vector plots for the 1550 nm design with dimensions $\mathrm{L} = 800\,\mathrm{nm}$, $\mathrm{w_x} = 520\,\mathrm{nm}$, $\mathrm{thx} = 90\,\mathrm{nm}$, $\mathrm{w_y} = 160\,\mathrm{nm}$, $\mathrm{thy} = 180\,\mathrm{nm}$, $\mathrm{dx} = 110\,\mathrm{nm}$, and $\mathrm{h} = 160\,\mathrm{nm}$. The transparent material is silicon and the lossy material is nickel as in Fig. 1, (d) Same as in (c), for the 532 nm design, with dimensions $\mathrm{L} = 520\,\mathrm{nm}$, $\mathrm{w_x} = 410\,\mathrm{nm}$, $\mathrm{thx} = 100\,\mathrm{nm}$, $\mathrm{w_y} = 110\,\mathrm{nm}$, $\mathrm{thy} = 90\,\mathrm{nm}$, $\mathrm{dx} = 40\,\mathrm{nm}$, and $\mathrm{h} = 160\,\mathrm{nm}$. The transparent material is sapphire, while the lossy material is nickel as in Fig. 2. In (c) and (d), the brackets [m, l] denote transmission orders.

orders in certain directions, while enhancing the remaining orders, we again employ Fourier analysis. In this case, the complex refractive index distribution $n\left(x,y\right) = f\left(x,y\right) + ig(x,y)$ is to be periodic on the surface of the PT-symmetric structure, where $f\left(x,y\right)$, $g\left(x,y\right)$ are real periodic functions, with spatial periods L_x, L_y along the x-axis and y-axis respectively. The parameters L_x, L_y physically represent the dimensions of each unit cell on the PT-symmetric metasurface in the x-direction and y-direction, correspondingly. By expanding $n\left(x,y\right)$ into a 2-D Fourier series we obtain

$$n\left(x,y\right) = \frac{1}{2}\sum_{m,l=0}^{\infty}\left\{\left[\left(a_{m,l}+c'_{m,l}\right)+i\left(a'_{m,l}-c_{m,l}\right)\right]e^{im\theta_x}e^{il\theta_y}\ +\right.$$

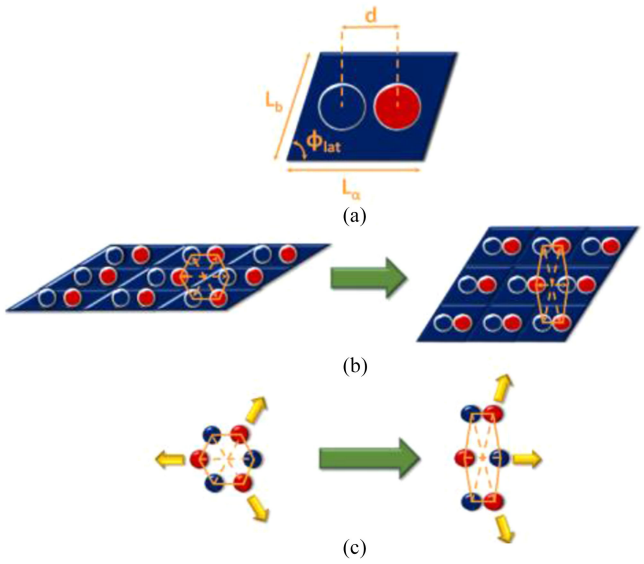

Fig. 4. (a) Unit cell of the diatomic oblique Bravais lattice, (b) geometric transformation from the honeycomb lattice (left), to the diatomic oblique Bravais lattice (right), and (c) corresponding transmission orders.

$$\left[\left(a_{m,l}-c'_{m,l}\right)+i\left(a'_{m,l}+c_{m,l}\right)\right]e^{-im\theta_x}e^{-il\theta_y}+$$
$$\left[\left(b_{m,l}+d'_{m,l}\right)+i\left(b'_{m,l}-d_{m,l}\right)\right]e^{im\theta_x}e^{-il\theta_y}+$$
$$\left[\left(b_{m,l}-d'_{m,l}\right)+i\left(b'_{m,l}+d_{m,l}\right)\right]e^{-im\theta_x}e^{il\theta_y}\Big\} \quad (4)$$

where $\theta_x=\frac{2\pi x}{L_x}$, $\theta_y=\frac{2\pi y}{L_y}$. In Eq. (4) $\{a_{m,l},b_{m,l},c_{m,l},d_{m,l}\}$ and $\{a'_{m,l},b'_{m,l},c'_{m,l},d'_{m,l}\}$ are the Fourier coefficients of the functions $f(x,y)$ and $g(x,y)$, respectively.

In order to achieve a unidirectional deflection, i.e., a suppression of the diffraction orders in all three quadrants $(e^{-im\theta_x}e^{il\theta_y},e^{-iml}e^{-il\theta_y},e^{im\theta_x}e^{-il\theta_y})$ except for the first $(e^{im\theta_x}e^{il\theta_y})$, the relations $c'_{m,l}=a_{m,l}$, $a'_{m,l}=-c_{m,l}$, $b_{m,l}=d'_{m,l}=b'_{m,l}=d_{m,l}=0$ should hold. Consequently, $f(x,y),g(x,y)$ take the form

$$f(x,y)=\sum_{m,l=0}^{\infty}\left\{a_{m,,l}\cos\left(m\frac{2\pi x}{L_x}+l\frac{2\pi y}{L_y}\right)+c_{m,l}\sin\left(m\frac{2\pi x}{L_x}+l\frac{2\pi y}{L_y}\right)\right\}$$
$$g(x,y)=\sum_{m,l=0}^{\infty}\left\{a_{m,l}\sin\left(m\frac{2\pi x}{L_x}+l\frac{2\pi y}{L_y}\right)-c_{m,l}\cos\left(m\frac{2\pi x}{L_x}+l\frac{2\pi y}{L_y}\right)\right\}. \quad (5)$$

From Eqs. (5), we conclude that the index distribution $n(x,y)$ is PT-symmetric, when the $a_{m,l},c_{m,l}$ terms in Eq. (5) are separately considered. These coefficients were imposed on 2-D scattering configurations and optimized using FEM.

We next define the reciprocal lattice vectors as $\overrightarrow{G_1}=2\pi(\overrightarrow{a_2}\times\vec{z})/\{\overrightarrow{a_1}\cdot(\overrightarrow{a_2}\times\vec{z})\}$ and $\overrightarrow{G_2}=2\pi(\vec{z}\times\overrightarrow{a_1})/\{\overrightarrow{a_1}\cdot(\overrightarrow{a_2}\times\vec{z})\}$, where $\overrightarrow{a_1}$, $\overrightarrow{a_2}$ are the unit cell vectors, while $\vec{z}$ is the unit vector along the z-axis, normal to the considered unit cell. The diffraction orders supported by the metasurface system can be determined from $\vec{k}_{diff,||}=\vec{k}_{inc,||}+m\overrightarrow{G_1}+l\overrightarrow{G_2}$, where the pair of integers $[m,l]$, represents the transmission order, $\vec{k}_{diff,||}$ and $\vec{k}_{inc,||}$ denote the tangential components of the diffracted and incident wave vector, respectively. The normal component of the diffracted wave vector can be found from $\vec{k}_{diff,\perp}=\sqrt{(k_0n_2)^2-|\vec{k}_{diff,||}|^2}\,\vec{z}$, where n_2 is the refractive index in the transmission medium. Finally the corresponding elevation and azimuth propagation angles can be evaluated from $\theta=\cos^{-1}(k_{diff,z}/k_0n_2)$ and $\varphi=\tan^{-1}(k_{diff,y}/k_{diff,x})$ respectively, where $k_{diff,x}$, $k_{diff,y}$ and $k_{diff,z}$ are the $x-$, $y-$ and $z-$ components of the diffracted wave vector.

B. PT-Symmetric H-Like Designs

We next consider the diffraction behavior of a 2-D PT-symmetric metasurface comprised of H-like elements (see Fig. 3). Such metasurface is locally and globally PT -symmetric around a central point. These designs are investigated for the wavelengths of 1550 and 532 nm using FEM. As in the 1-D case, the materials considered here are silicon and nickel (1550 nm), while for the 532 nm design are sapphire and nickel. Given that each H-like element is passively PT-symmetric [see Fig. 3(a)], one expects that the entire metasurface will exhibit this same symmetry. In performing FEM simulations, we assume normal incidence with the electric field linearly polarized along the y-axis. Based on the chosen dimensions and the wavelength of operation, we deduce that these configurations support up to eight transmission orders.

For the 1550 nm design, the extinction ratio is 65 (18 dB) between the [1, 1] and $[-1,-1]$ transmission orders [see Fig. 3(c)] when the loss of nickel is taken into account (PT-symmetric metasurface). This is in stark contrast to its corresponding Hermitian design, where the ratio is unity and the transmitted field distribution is completely symmetric. This same ratio is approximately 11 for the [0, $\pm$1] orders and 6 for the [$\pm$1, 0] orders. In Fig. 3(c) an overall deflection of the near field is observed in the $y=0$, $x=0$ and $x=y$ planes, which stems from the significant asymmetry in the diffraction efficiencies of the transmission order pairs $\{[1,0],[-1,0]\}$, $\{[0,1],[0,-1]\}$, $\{[1,1],[-1,-1]\}$. This strong asymmetry arises from the fact that the lossy material is mostly present in the first quadrant, while it is completely absent from the third. On the other hand, even though the lossy material is equally distributed in the second and fourth quadrants it still leads to reduced efficiencies to the transmission orders $[-1,1]$, $[1,-1]$ that happen to be below 1%.

Similar results are obtained for the 532 nm design. The extinction ratio between the [1, 1] and $[-1,-1]$ transmission orders reaches up to a value of 65, while for the [0, $\pm$1] orders and [$\pm$1, 0] orders is 12 and 10 respectively [see Fig. 3(d)]. Field distributions and Poynting vector plots, as obtained from FEM, are also shown in this same figure.

We know that this suppression/enhancement behavior is a direct result of the judicious distribution of transparent and lossy elements on this metasurface. As we will see in the next section, such diffractive elements can be arranged in a different manner, while still retaining the overall PT-symmetric characteristics.

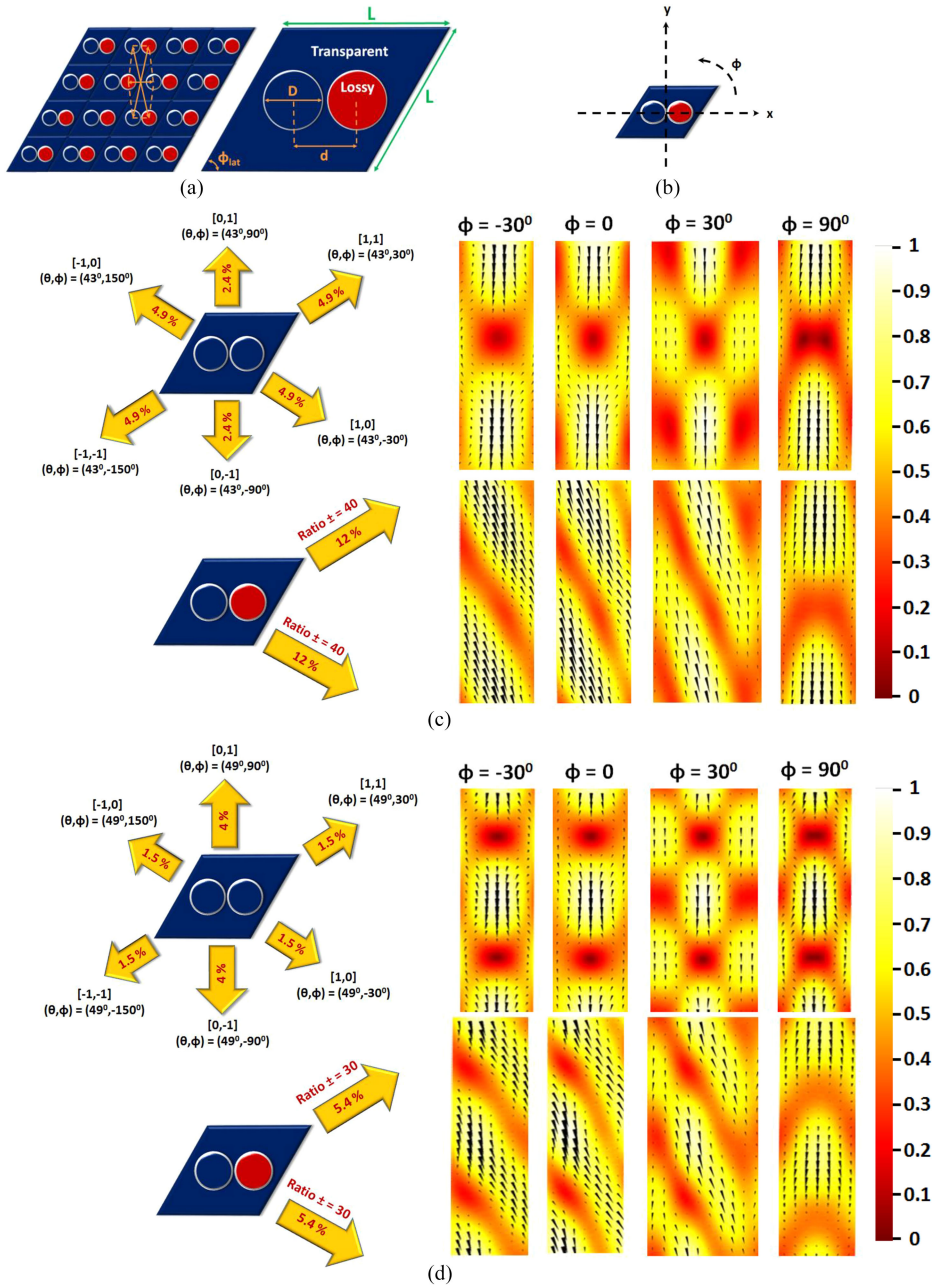

Fig. 5. Oblique diatomic Bravais lattice design: (a) unit cell and corresponding lattice, (b) coordinate plane, (c) FEM results of the transmission order efficiencies, normalized near-field distributions and Poynting vector plots for the 1550 nm design with dimensions L = 750 nm, D = 260 nm, d = 290 nm, h = 330 nm, and $\phi_{lat} = 60°$. The materials and respective refractive indices are the same as in Fig. 1, (d) FEM results of the diffraction efficiencies, normalized near-field distributions and Poynting vector plots for the 532 nm design with dimensions L = 460 nm, D = 160 nm, d = 180 nm, h = 330 nm, and $\phi_{lat} = 60°$. The materials and respective refractive indices are the same as in Fig. 2. In (c), and (d), the brackets [m, l] denote transmission orders.

C. PT-Symmetric Diatomic Oblique Bravais Lattice Designs

In this section we use an oblique Bravais PT lattice design in order to achieve unidirectional deflection in the diffraction orders of this metasurface. To do so, we utilize a diatomic configuration, similar to that shown in Fig. 4. The various quantities associated with this system are L_a, L_b, d, and φ_{lat} [see Fig. 4(a)].

In its Hermitian manifestation, such a honeycomb system will symmetrically excite the diffraction orders. Even if PT-symmetry is passively imposed and therefore some of the orders are eliminated [see Fig. 4(c)], the diffraction is still angularly balanced under normal incidence. Hence, in order to enhance some of the orders at the expense of others, the PT diatomic cell must assume an oblique shape with an angle φ_{lat} above 30°. This latter necessity arises from geometric considerations. More specifically, the honeycomb lattice [see Fig. 4(b)] is characterized by the relations $L_a = 2 * L_b * \cos(\varphi_{lat}), L_b = 2 * d * \cos(\varphi_{lat})$ and $\varphi_{lat} = 30°$. Given the underlying symmetry of a honeycomb lattice, even in the PT-symmetric case, we don't observe directional scattering towards a particular angular sector. In order to break this spatial symmetry, we have relaxed the requirement $L_b = 2 * d * \cos(\varphi_{lat})$ to

$L_b/(2 * d * \cos(\varphi_{lat})) > 2$. FEMs indicate that under these conditions, orders propagating in a particular angular sector can be enhanced, while the rest are eliminated. In the examples that follow we use $\varphi_{lat} = 60^\circ$. Note that under this oblique transformation, the PT-symmetry condition is still retained in each cell and in the lattice in general.

For the sake of comparison, two designs are again analyzed at 1550 and 532 nm. In both cases, the same materials are used as in Section III-B. Here we assume normal incidence, with the electric field linearly polarized in the horizontal direction [azimuthal plane $\varphi = 0$, Fig. 5(b)]. Under these conditions, the simulated structures support six transmission orders.

For the 1550 nm design [see Fig. 5(c)], the extinction ratio between the rightward [1, 1], [1, 0] and the respective leftward orders [−1, −1], [−1, 0] is approximately 40 (16 dB) when loss is employed (PT-symmetric case). Such an asymmetry in the diffraction efficiencies justifies the strong bending of the near field in the azimuthal planes $\varphi = 0$, $\varphi = 30$ and $\varphi = -30$. On the other hand, in the azimuthal plane $\varphi = 90$ no deflection occurs. The diffraction efficiencies of the transmission orders [0, ±1] propagating in the same plane, are much less than 1% and thus do not alter the propagation of the power flow. Similar effects are observed for the 532 nm design [see Fig. 5(d)]. More specifically, in the PT-symmetric case the extinction ratios between the rightward [1, 1], [1, 0] and the respective leftward orders [−1, −1], [−1, 0] scales up to 30 (15 dB), which results in the asymmetric scattering of the near field in the azimuthal planes $\varphi = 0$, $\varphi = 30$ and $\varphi = -30$. Instead in the azimuthal plane $\varphi = 90$ the scattering pattern remains symmetric since the diffraction efficiencies of the propagating orders [0, ±1] are reduced to much below 1%.

IV. Concluding Remarks

In conclusion, we have shown that by merging two recently developed concepts, those associated with PT-symmetry and metasurface optics, one can design systems with highly directional scattering characteristics. Passive PT-symmetry can be readily introduced in these arrangements by judiciously exploiting loss. In this study, all-passive one-dimensional and two-dimensional metasurface designs have been investigated. In two-dimensional settings, we have shown that PT symmetry can be established by employing either H-like diffractive elements or diatomic oblique Bravais lattices. PT-symmetric metasurfaces can provide an alternative avenue to existing techniques for effectively manipulating the resulting diffraction orders through surface-confined passive nano-features.

References

[1] C. M. Bender and S. Boettcher, "Real spectra in non-hermitian hamiltonians having PT symmetry," *Phys. Rev. Lett.*, vol. 80, no. 24, pp. 5243–5246, 1998.

[2] K. G. Makris, R. El-Ganainy, D. N. Christodoulides, and Z. H. Musslimani, "Beam dynamics in PT symmetric optical lattices," *Phys. Rev. Lett.*, vol. 100, 2008, Art. no. 103904.

[3] C. E. Rüter *et al.*, "Observation of parity-time symmetry in optics," *Nat. Phys.*, vol. 6, pp. 192–195, 2010.

[4] A. Guo *et al.*, "Observation of PT-symmetry breaking in complex optical potentials," *Phys. Rev. Lett.*, vol. 103, 2009, Art. no. 093902.

[5] S. Longhi, "Bloch oscillations in complex crystals with PT symmetry," *Phys. Rev. Lett.*, vol. 103, 2009, Art. no. 123601.

[6] H. Hodaei, M. A. Miri, M. Heinrich, D. N. Christodoulides, and M. Khajavikhan, "Parity- time symmetric microting lasers," *Science*, vol. 346, no. 6212, pp. 975–978, 2014.

[7] L. Feng, Z. J. Wong, R.-M. Ma, Y. Wang, and X. Zhang, "Single-mode laser by parity-time symmetry breaking," *Science*, vol. 346, pp. 972–975, 2014.

[8] H. Ramezani, D. N. Christodoulides, V. Kovanis, I. Vitebskiy, and T. Kottos, "PT-symmetric talbot effects," *Phys. Rev. Lett.*, vol. 109, 2012, Art. no. 033902.

[9] T. Kottos, "Optical physics: Broken symmetry makes light work," *Nature Phys.*, vol. 6, pp. 166–167, 2010.

[10] S. Klaiman, U. Günther, and N. Moiseyev, "Visualization of branch points in PT-symmetric waveguides," *Phys. Rev. Lett.*, vol. 101, 2008, Art. no. 080402.

[11] B. Peng *et al.*, "Parity-time symmetric whispering gallery microcavities," *Nat. Phys.*, vol. 10, pp. 394–398, 2014.

[12] A. Regensburger *et al.*, "Parity-time synthetic photonic lattices," *Nature*, vol. 488, pp. 167–171, 2012.

[13] Z. Lin *et al.*, "Unidirectional invisibility induced by PT -symmetric periodic structures," *Phys. Rev. Lett.*, vol. 106, 2011, Art. no. 213901.

[14] G. Castaldi, S. Savoia, V. Galdi, A. Alù, and N. Engheta, "PT metamaterials via complex-coordinate transformation optics," *Phys. Rev. Lett.*, vol. 110, 2013, Art. no. 173901.

[15] N. Yu and F. Capasso, "Flat optics with designer metasurfaces," *Nature Mater.*, vol. 13, pp. 139–150, 2014.

[16] A. V. Kildishev, A. Boltasseva, and V. M. Shalaev, "Planar photonics with metasurfaces," *Science*, vol. 339, no. 6125, 2013, Art. no. 1232009.

[17] S. Larouche and D. R. Smith, "Reconciliation of generalized refraction with diffraction theory," *Opt. Lett.* vol. 37, pp. 2391–2393, 2012.

[18] N. Yu *et al.*, "Light propagation with phase discontinuities: Generalized laws of reflection and refraction," *Science*, vol. 334, no. 6054, pp. 333–337, 2011.

[19] F. Aieta *et al.*, "Out-of-plane reflection and refraction of light by anisotropic optical antenna metasurfaces with phase discontinuities," *Nano Lett.*, vol. 12, pp. 1702–1706, 2012.

[20] P. Genevet *et al.*, "Ultra-thin plasmonic optical vortex plate based on phase discontinuities," *Appl. Phys. Lett.*, vol. 100, 2012, Art. no. 013101.

[21] R. Blanchard *et al.*, "Modeling nanoscale V-shaped antennas for the design of optical phased array," *Phys. Rev. B*, vol. 85, 2012, Art. no. 155457.

[22] F. Aieta *et al.*, "Aberration-free ultrathin flat lenses and axicons at telecom wavelengths based on plasmonic metasurfaces," *Nano Lett.*, vol. 12, pp. 4932–4936, 2012.

[23] Y. Ra'di, V. S. Asadchy and S. A. Tretyakov, "Total absorption of electromagnetic waves in ultimately thin layers," *IEEE Trans. Antennas Propag.*, vol. 61, no. 9, pp. 4606–4614, Sep. 2013.

[24] V. S. Asadchy, Y. Ra'di, J. Vehmas, and S. A. Tretyakov, "Functional metamirrors using bianisotropic elements," *Phys. Rev. Lett.*, vol. 114, 2015, Art. no. 095503.

[25] L. Poladian, "Resonance mode expansions and exact solutions for nonuniform gratings," *Phys. Rev. E.*, vol. 54, pp. 2963–2975, 1996.

[26] M. V. Berry, "Lop-sided diffraction by absorbing crystals," *J. Phys. Math. Gen.*, vol. 31, pp. 3493–3502, 1998.

[27] R. Birabassov, A. Yesayan, and T. V. Galstyan, "Nonreciprocal diffraction by spatial modulation of absorption and refraction," *Opt. Lett.*, vol. 24, pp. 1669–1671, 1999.

[28] N. X. A. Rivolta and B. Maes, "Diffractive switching by interference in a tailored PT-symmetric grating," *J. Opt. Soc. Amer. B*, vol. 32, pp. 1330–1337, 2015.

[29] S. Phang, A. Vukovic, H. Susanto, T. M. Benson, and P. Sewell "Ultrafast optical switching using parity–time symmetric Bragg gratings," *J. Opt. Soc. Amer. B*, vol. 30, pp. 2984–2991, 2013.

[30] M. Kulishov, H. F. Jones, and B. Kress, "Analysis of PT-symmetric volume gratings beyond the paraxial approximation," *Opt. Express*, vol. 23, no. 7, pp. 9347–9362, 2015.

[31] M. Kulishov and B. Kress, "Free space diffraction on active gratings with balanced phase and gain/loss modulations," *Opt. Express*, vol. 20, pp. 29319–29328, 2012.

[32] R. Fleury, D. L. Sounas, and A. Alù, "Negative refraction and planar focusing based on parity-time symmetric metasurfaces," *Phys. Rev. Lett.*, vol. 113, 2014, Art. no. 023903.

[33] Y. Jia, Y. Yan, S. V. Kesava, E. D. Gomez, and N. C. Giebink, " Passive parity-time symmetry in organic thin film waveguides," *ACS Photon.*, vol. 2, no. 2, pp. 319–325, 2015.

[34] Y. Yan and N. C. Giebink, "Passive PT symmetry in organic composite films via complex refractive index modulation," *Adv. Opt. Mater.*, vol. 2, no. 5, pp. 423–427, 2014.
[35] H. Kogelnik, "Coupled wave theory for thick hologram gratings," *Bell Syst. Tech. J.*, vol. 48, pp. 2909–2947, 1969.
[36] M. G. Moharam, and T. K. Gaylord, "Diffraction analysis of dielectric surface-relief gratings," *J. Opt. Soc. Amer.*, vol. 72, pp. 1385–1392, 1982.
[37] J. Albero *et al.*, "Generalized diffractive optical elements with asymmetric harmonic response and phase control" *Appl. Opt.*, vol. 52, pp. 3637–3644, 2013.
[38] H. H. Li, "Refractive index of silicon and germanium and its wavelength and temperature derivatives," *J. Phys. Chem. Ref. Data*, vol. 9, no. 3, pp. 561–658, 1980.
[39] A. D. Rakić, A. B. Djurišić, J. M. Elazar, and M. L. Majewski, "Optical properties of metallic films for vertical-cavity optoelectronic devices," *Appl. Opt.*, vol. 37, pp. 5271–5283, 1998.
[40] I. H. Malitson, "Refraction and Dispersion of Synthetic Sapphire," *J. Opt. Soc. Amer.*, vol. 52, pp. 1377–1379, 1962.

Nicholas S. Nye received the bachelor's and master's degrees in electrical engineering physics from the Aristotle University of Thessaloniki, Thessaloniki, Greece, in 2011 and 2012, respectively. He joined CREOL-the College of Optics and Photonics, University of Central Florida, Orlando, FL, USA, in 2013, and received the master's degree in optics and photonics in 2014. He is currently working toward the Ph.D. degree in optics and photonics in CREOL. His research interests include optical metasurfaces, nonlinear optics, beam shaping, optical solitons, and parity-time symmetric synthetic devices.

Ahmed El Halawany received the bachelor's and master's degrees in theoretical physics from the American University in Cairo, New Cairo, Egypt, in 2006 and 2008, respectively. In 2010, he received the master's degree from the University of Central Florida, Orlando, FL, USA. He is currently working toward the Ph.D. degree in physics from the University of Central Florida.

Ahmed Bakry received the M.Sc. degree from the University of Arizona, Tucson, AZ, USA, in theoretical physics in 1985, the diploma degree in analytical physics in 1991, and the Ph.D. degree in laser physics from the University of Wales , Cardiff, U.K., in 1994. He is the Director of Laser Applications Group, King Abdulaziz University and currently working at Physics Department on dynamics and noise in semiconductor lasers, diagnosis of cancer by laser induced fluorescence, nonlinear optical properties of novel organic dyes, and inorganic thin films.

M. A. N. Razvi received the M.Sc. degree from Osmania University, Hyderabad, India, in 1980, and the Ph.D. degree from the University of Bombay, Mumbai, India, in 1994, in physics. He was with the Spectroscopy Division, Bhabha Atomic Research Centre, Mumbai, India, from 1982 to 2007, on laser spectroscopy of atoms and small molecules, laser mass spectrometry, multiphoton ionization, development of MALDI and RIMS, study of proteins. He is currently with Physics Department, King Abdulaziz University, Jeddah, Saudi Arabia, on diagnosis of cancer by laser induced fluorescence, and nonlinear optical properties of novel organic dyes and inorganic thin films.

Ahmed Alshahrie received the bachelor's (B.Sc.) degree in physics in 2001, the master's (M.Phil.) degree in experimental laser spectroscopy, his thesis was entitled "Nano-second laser source for use in analytical spectroscopy" from University of Wales, Swansea, U.K., in 2007. In 2011, he received the Ph.D. degree from Swansea University, Swansea, U.K., his thesis was entitles "Raman Spectroscopy of hydrogen isotopologues and trace gas analysis for KATRIN." He is currently an Assistant Professor at Physics Department, King AbdulAziz University, Jeddah, Kingdom of Saudi Arabia, the Deputy Director of the Nanotechnology Centre, King AbdulAziz University from 1st June 2015 till now.

Mercedeh Khajavikhan received the B.S. and M.S. degrees in electronics from the Amirkabir University of Technology, Tehran, Iran, in 2000 and 2003, respectively, and the Ph.D. degree in electrical engineering from the University of Minnesota, Minneapolis, MN, USA, in 2009. Her Ph.D. dissertation was on coherent beam combining for high-power laser applications. In 2009, she joined the University of California in San Diego as a Post-Doctoral Researcher where she worked on the design and development of nanolasers, plasmonic devices, and silicon photonics components. In August 2012, she joined the College of Optics and Photonics, University of Central Florida as an Assistant Professor. In 2015, she received NSF Early CAREER Award.

Demetrios N. Christodoulides received the Ph.D. degree from The Johns Hopkins University, Baltimore, MD, USA, in 1986. He is the Cobb Family Endowed Chair and Pegasus Professor of Optics at the College of Optics and Photonics, University of Central Florida. He subsequently joined Bellcore as a Post-Doctoral Fellow at Murray Hill. Between 1988 and 2002, he was with the Faculty of the Department of Electrical Engineering, Lehigh University. His research interests include linear and nonlinear optical beam interactions, synthetic optical materials, optical solitons, and quantum electronics. His research initiated new innovation within the field, including the discovery of optical discrete solitons, Bragg and vector solitons in fibers, nonlinear surface waves, and the discovery of self-accelerating optical (Airy) beams. He has authored and coauthored more than 300 papers. He is a Fellow of the Optical Society of America and the American Physical Society. In 2011, he received the R.W. Wood Prize of OSA.